4th IASPEI / IAEE International Symposium:

Effects of Surface Geology on Seismic Motion

August 23–26, 2011 · University of California Santa Barbara

PERIOD-DEPENDENT SITE AMPLIFICATION FOR THE 2008 IWATE-MIYAGI NAIRIKU, JAPAN, EARTHQUAKE SEQUENCE

Rami Ibrahim
Earthquake Research Institute,
University of Tokyo,
Japan

Kazuki Koketsu
Earthquake Research Institute,
University of Tokyo,
Japan

Hiroe Miyake
Earthquake Research Institute,
University of Tokyo,
Japan

ABSTRACT

Site amplification factors at period ranges of 0.1-0.2, 0.2-0.3, 0.3-0.5, 0.5-1, 1-2, and 2-10 s were determined for 27 stations of KiK-net and K-NET in and around the source area of the 2008 Iwate-Miyagi Nairiku earthquake. The ratio of the geometric mean values of the two maximum horizontal amplitudes of acceleration and velocity at the uphole to that at the downhole is considered as the amplification factor of KiK-net stations. The bedrock borehole ground motions of KiK-net were used as the reference motions to get the amplification factors for K-NET stations. Amplification factors of 3 to 33 at short- period ranges of 0.1 to 0.3 s are observed at many stations such as AKTH04, IWTH22, MYG004, and so on. The stations of MYG004, MYG005, and MYG006 have shown amplification factors of 3 to 8 at long- period ranges of 1 to 10 s. On the other hand, AKT023, IWT010, and IWT011 stations show flat response spectra compared to hard rock sites. Larger acceleration amplification than velocity amplification is observed at stations located on deep soft soil structures such as MYG004, MYG006, and YMT006. The results are compared to other results by H/H and H/V spectral ratios of the mainshock and five aftershocks data.

INTRODUCTION

The 2008 Iwate-Miyagi Nairiku earthquake on 14 June 2008 mainly struck the Tohoku region, northeastern Japan. The JMA magnitude was determined at M_{JMA} 7.2 by Japan Meteorological Agency (JMA), and the moment magnitude by the Global CMT project was at M_w 6.9. Reverse fault type was dominated for this event. The epicenter was located at 39.025 N 140.883 E and the depth at 8 km by the National Research Institute for Earth Science and Disaster Prevention (NIED). The fault plane extends to 40km in the strike direction (N209°E) and 18 km in the dip direction (40°) (Suzuki et al., 2010) (Fig 1). This earthquake has attracted the interest in seismology and earthquake engineering. Aoi et al. (2008) show the trampoline effect at the vertical component of IWTH25 station which caused for upward amplitude up to 33.66 m/s^2. The station itself is located 3 km to the south of epicenter was recorded the largest ground acceleration to date of 40.22 m/s^2 (vector sum of three orthogonal components). Motoki et al. (2010) studied the reason of the long- period ground motion at the Onikoke region located in the south of source area. We also noticed some features from the acceleration and velocity spectral maps of this earthquake at some periods, we will discuss more details later. Generally, the amplification factor is calculated by either spectral ratio or Fourier ratio between free surface and bedrock. The method does not differentiate between PGA or PGV amplification considering the same value for both parameters. The surface geology is shown to effect more on amplification of PGA than of that of PGV. Amplification ratio of PGA has a tendency to decrease as input motion increases. This phenomenon is clear where liquefaction occurs (soft deposit sites). The decrease of PGV amplification hardly occurs even if liquefaction occurs (Suetomi et al., 2004). Seismic hazard assessment maps depend mainly on empirical relation of PGV on the bedrock. In this study, we try to check whether the PGA and PGV amplification factors have some differences in case of the 2008 Iwate-Miyagi Nairiku earthquake. The good distribution of seismic stations around the source area with borehole recorders enabled us to find good reference sites to study the site amplification. We propose to calculate the site amplification factor directly from acceleration and velocity time series between the surface and downhole stations. First, we applied filtering technique in period ranges of 0.1-0.2, 0.2-0.3, 0.3-0.5, 0.5-1, 1-2, and 2-10s. Then we get the amplification factor as the ratio of geometric mean value of the maximum horizontal components at the uphole to the downhole. Finally we compare our results to those from other methods such as H/H and H/V spectral ratios of the mainshock and five aftershocks data.

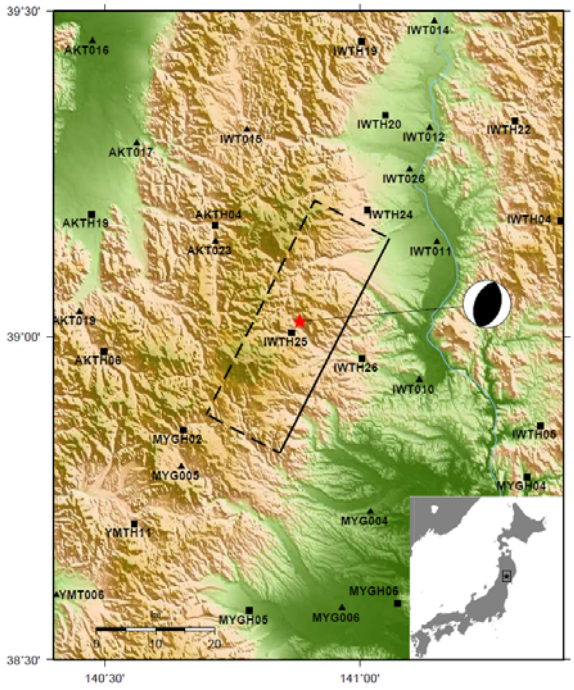

Fig. 1. The topographic map of the source region of the 2008 Iwate-Miyagi Nairiku earthquake. Inset shows studied area (black frame). Red star indicates epicenter of the mainshock determined by NIED. The black rectangle indicates the surface projection of the fault plane (Suzuki et al., 2010). Solid line indicates the upper edge of the fault. KiK-net stations are shown in black squares while K-NET stations in black triangles (strong motion network, NIED, Japan).

5% DAMPED ACCELERATION AND VELOCITY RESPONSE MAPS

We prepared 5% damped acceleration and velocity response spectra for 110 stations in and around the source area of the 2008 Iwate-Miyagi Nairiku earthquake. The data used for this study are strong motion data by KiK-net and K-NET (NIED). To show the spatial distribution of the response spectra we plot the acceleration and velocity amplitudes on maps for periods centered at 0.1, 0.2, 0.3, 0.5, 1, 2, 3, 5, and 10 s (Figs 2 and 3). The acceleration response spectra at source area show large amplitude in short periods and decrease in medium and longer periods. While the velocity response spectra amplitudes increase gradually from short periods to medium periods and decrease again at longer periods at the source area. AKTH04 station at the hanging- wall which is located far about 22 km to the north western part of the source area has large acceleration and velocity spectral amplitudes at 0.1 and 0.2 s and larger than recorded at source area at 0.3 s. Large acceleration spectral amplitudes is also extended far to the foot wall area at 0.1 s. Large velocity spectral amplitudes have recorded to the southern part of the source area at periods of 2, 3, 5 and 10 s at MYG005, MYG004 and MYG006 stations. Large velocity spectral amplitude is also recorded to the north western part of the source area in a period range of 3 and 5 s.

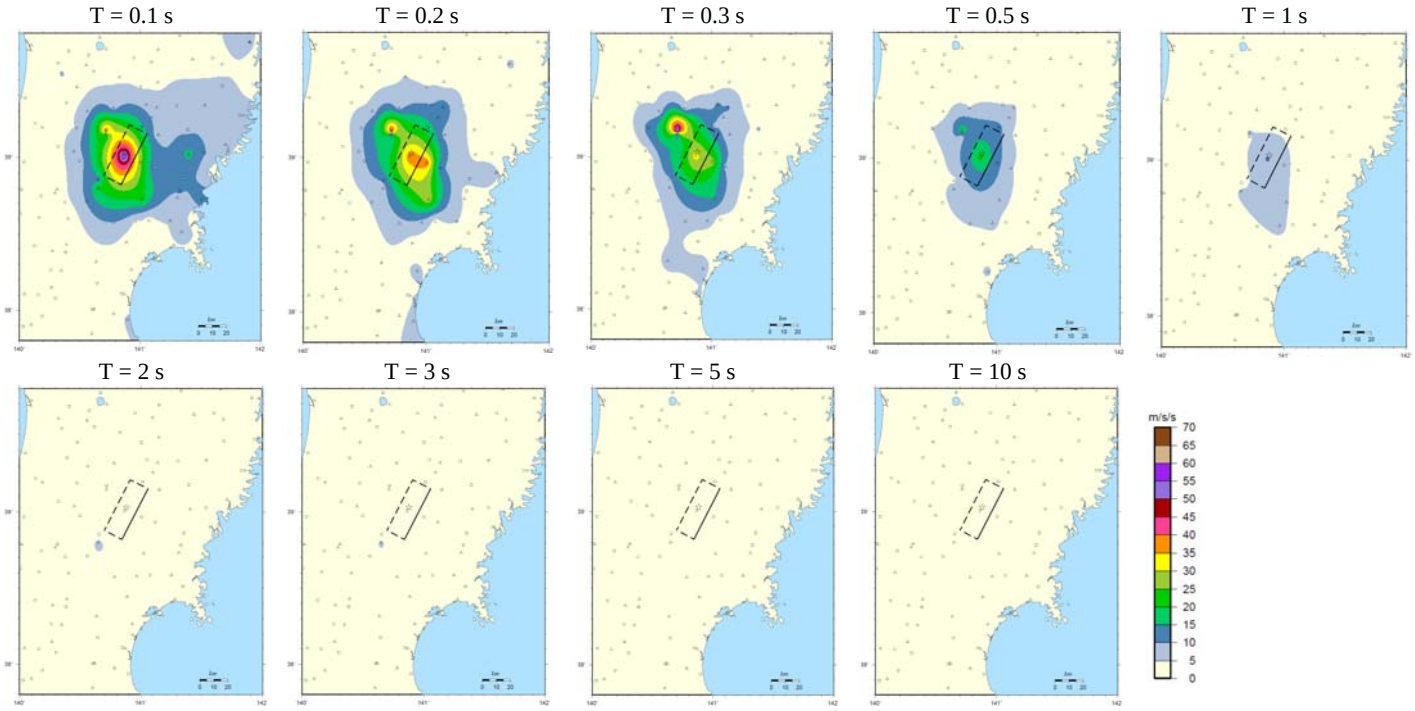

Fig. 2. 5% damped acceleration response spectra at 0.1, 0.2, 0.3, 0.5, 1, 2, 3, 5, and 10 s. Source area is shown in black rectangle (Suzuki et al., 2010). Large values at short periods of the source area decrease gradually at longer periods. Large values at AKTH04 North West of the source area at short periods. Foot wall area is also shown large amplitude extended far from the source area.

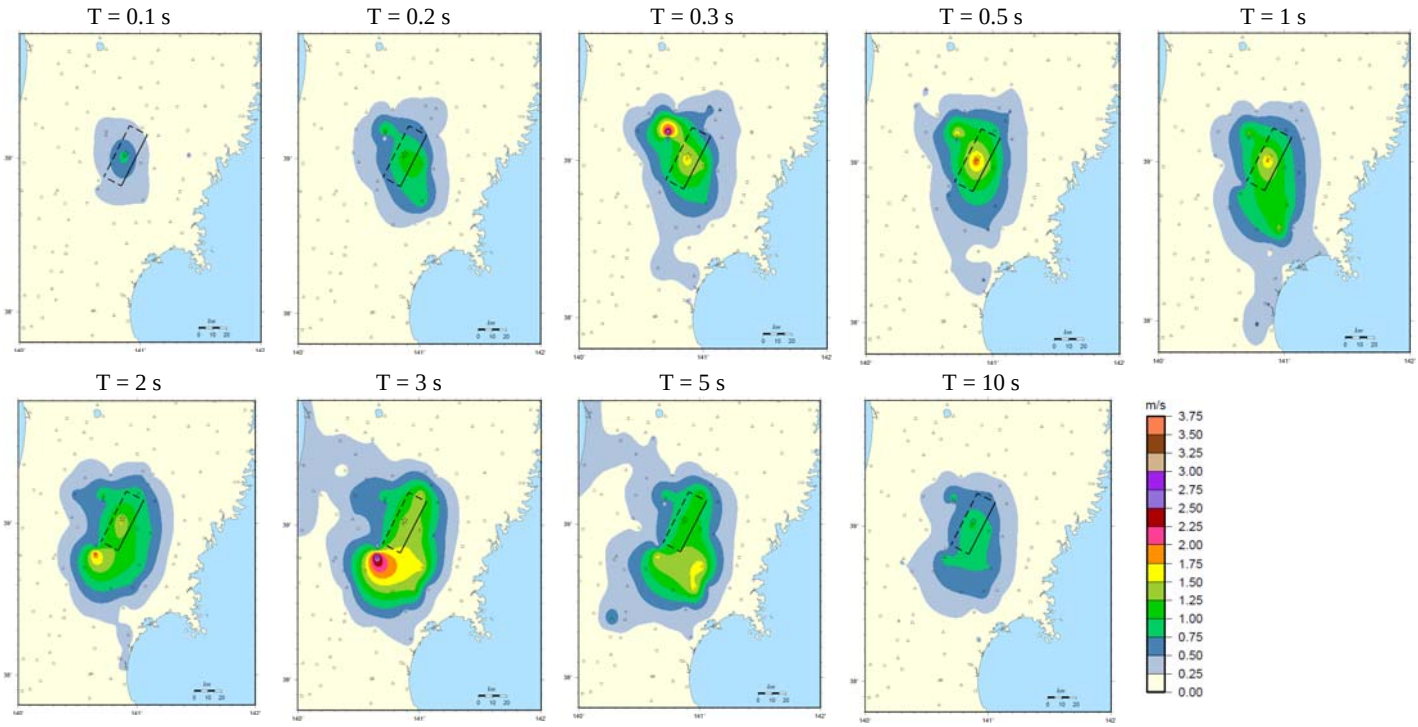

Fig. 3. 5% damped velocity response spectra at 0.1, 0.2, 0.3, 0.5, 1, 2, 3, 5, and 10 s. Source area is shown in black rectangle (Suzuki et al., 2010). Amplitude values increase gradually from short periods to medium periods and decrease again at longer periods at the source area. Large values at AKTH04 North West of the source area at short periods. Large values at the southern part of the source area at long periods. Large amplitudes at 2 and 3 s extended far to the west and North West of the source area.

ESTIMATION OF SITE AMPLIFICATION FACTORS

We estimated site amplification factors for 14 KiK-net and 13 K-NET stations. Each station of KiK-net has uphole and borehole accelerometers. The borehole depths range from 103-263 m. K-NET station has just one accelerometer at the free surface (Fig 1). The method we have used here to determine the amplification ratio depends on applying a filtering technique of the acceleration and velocity waveforms at different period ranges of 0.1-0.2, 0.2-0.3, 0.3-0.5, 0.5-1, 1-2, and 2-10 s (Fig 4). The geometric mean ratio from the maximum amplitude of the two horizontal components at surface and bottom is considered the amplification ratio in case of KiK-net data according to the equation (1).

$$amp = \frac{\sqrt{A_{NS_S} \times A_{EW_S}}}{\sqrt{A_{NS_B} \times A_{EW_B}}} \tag{1}$$

In the case of K-NET stations, the stations have just one accelerometer at the surface. It is necessary to compare K-NET surface data to reference sites. Therefore, the close KiK-net borehole stations is considered as reference sites taking into considerations the rock conditions at borehole basement. We could find nine stations which have shown good site conditions as they examined by H/V spectral ratio. Most stations show flat spectra and amplification factors between 1 and 2. These values reflect good conditions at the borehole basement to be considered as reference sites (Fig 5). Nine stations were selected as reference stations are shown in Fig 6. The bedrock borehole ground motion can be considered a good reference site for seismic hazard analysis even at distances as large as 20 km from the soil site (Steidl et al., 1996).

The correction for distance is also taken into account in the calculation of the amplification ratio. For that reason, we prepared local attenuation curves of the studied area within 100 km source distance (Fig 7). The attenuation curves were done using downhole KiK-net data for acceleration and velocity waveforms within same period ranges aforementioned. The geometric mean ratio from the maximum amplitude of the two horizontal components at surface and the reference station is considered the amplification ratio after adding the distance correction factor. So the amplification ratio is related to the below equation (2).

$$amp = \frac{\sqrt{A_{NS_S} \times A_{EW_S}}}{\sqrt{A_{NS_R} \times A_{EW_R}}} + c \quad (C\text{: distance correction factor}) \tag{2}$$

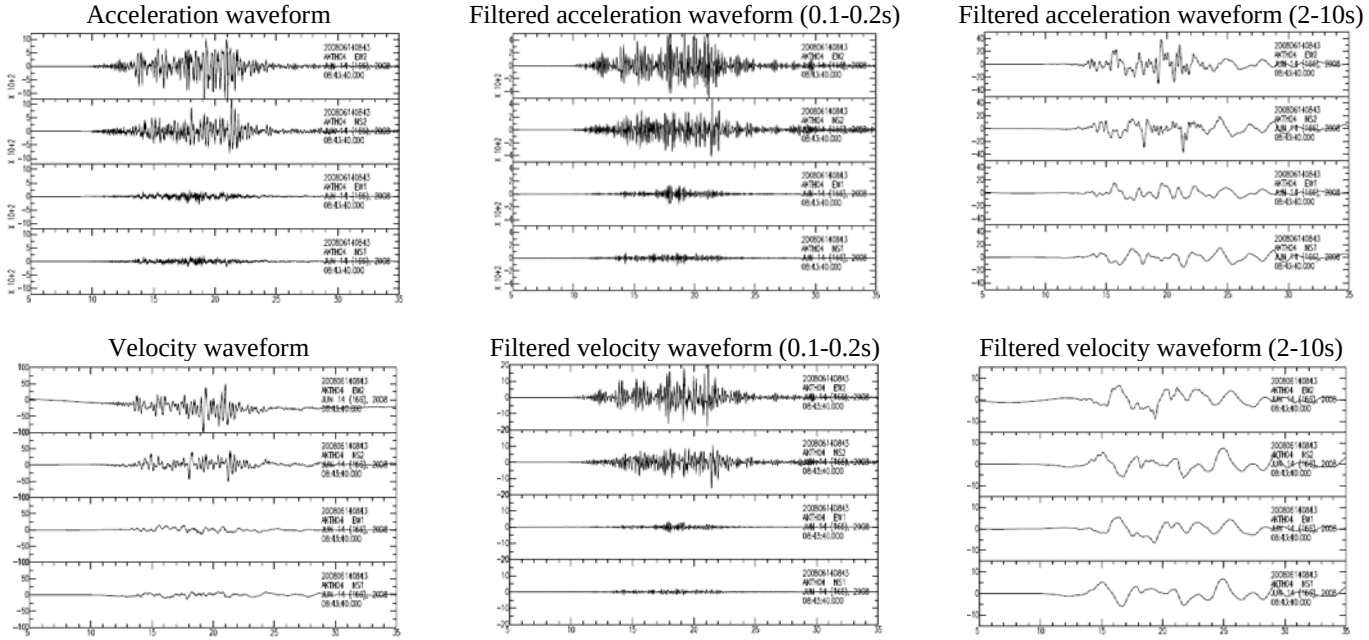

Fig. 4. Examples of the acceleration and velocity waveforms. Original waveforms are to the left. Middle figures show filtered waveforms at short period of 0.1-0.2 s, while the figures to the right show filtered waveforms at long periods of 2-10 s.

Table 1. Aftershock data used to calculate H/V spectral ratio

No.	Occurrence time					Latitude (N)	Longitude (E)	Depth (Km)	M_w
	Year	Month	Day	Hour	Minute				
1	2008	6	14	9	20	38.877	140.680	6	5.7
2	2008	6	14	10	40	38.927	140.888	6	4.8
3	2008	6	14	12	27	39.139	140.946	11	5.2
4	2008	6	14	23	42	38.992	140.893	10	4.8
5	2008	6	16	23	14	38.994	140.843	11	5.3

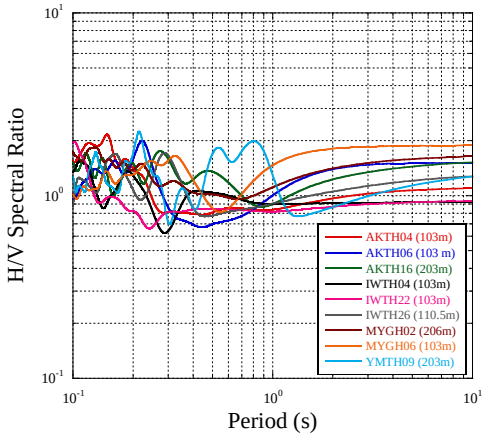

Fig. 5. The spectral ratio of H/V at the base rock of the borehole of reference sites of KiK-net. Flat response spectra refer to good rock conditions.

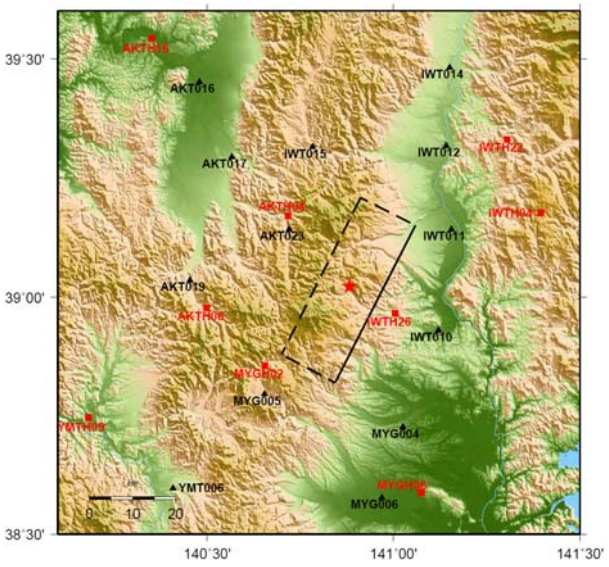

Fig. 6. K-NET stations used to calculate for amplification ratio in black triangles. KiK-net reference stations in red squares.

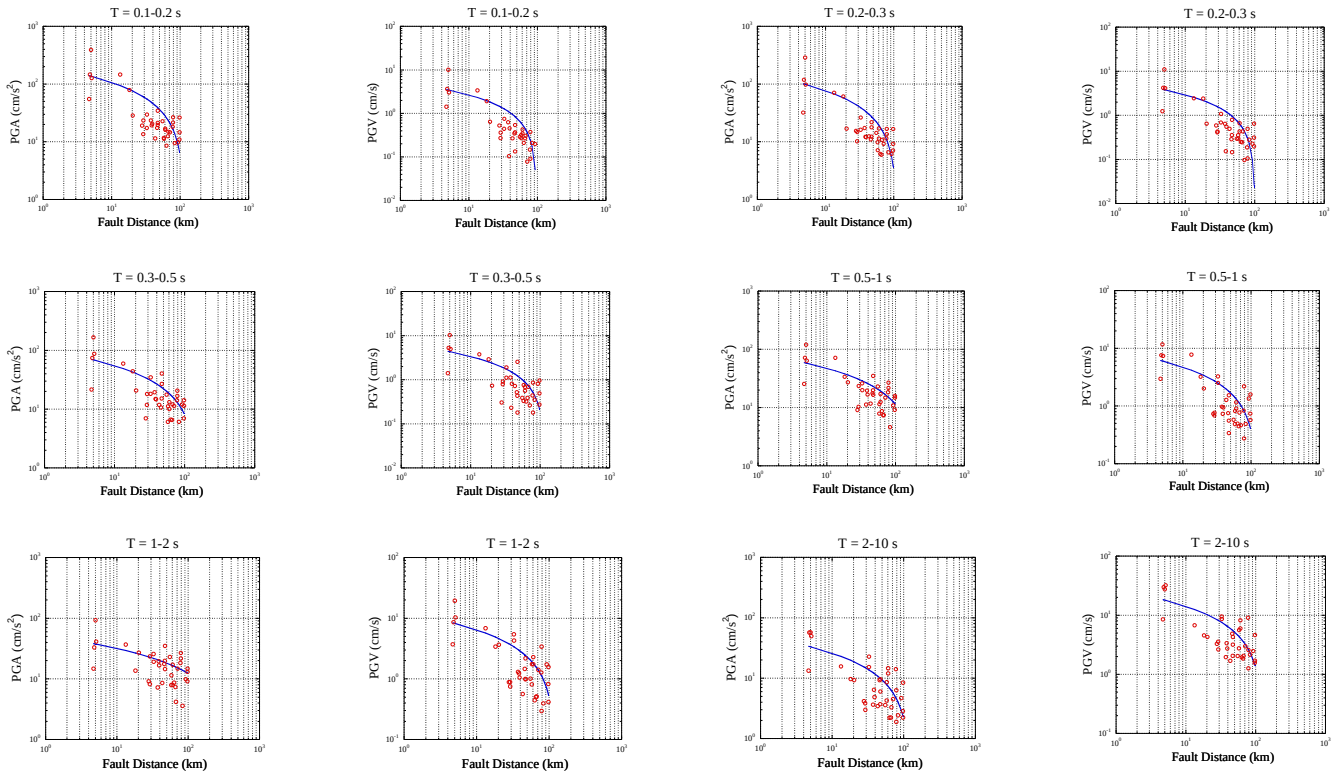

Fig. 7. The attenuation curves of PGA and PGV at 100 km fault distance at period ranges of 0.1-0.2, 0.2-0.3, 0.3-0.5, 0.5-1, 1-2, and 2-10 s. KiK-net borehole data were used to draw the attenuation curves. The curves were used for distance correction of the target stations and reference ones.

RESULTS AND DISCUSSION

The results of amplification ratio for KiK-net and K-NET stations are presented in Figs 8 and 9. Large amplification at short- periods and small amplification at long- periods are dominated for most KiK-net and some K-NET stations. Small amplifications at most periods which might be related to hard rock sites are appeared at some stations such as MYGH06, AKT023, IWT010, and so on. Amplification factor of approximately 13 and 33 at short- periods are shown at AKTH04 and MYG004, respectively. The velocity model of AKTH04 shows high *P*-wave and *S*-wave velocity contrast at a depth of 20 m. The *P*-wave velocity sharply decreases from 3000 m/s to 880 m/s while *S*-wave velocity decreases from 980 m/s to 430 m/s. The sudden change of velocity at such depth might be the reason of such Large amplification at short period ranges of 0.1-0.5 s. Unfortunately the velocity model of MYG004 is available just for the shallow depth up to 10 m. The model shows *P*-wave and *S*-wave velocity change at 5 m in depth. The *P*-wave decreases from 1800 m/s to 940 m/s while *S*-wave decreases from 550 m/s to 240 m/s. More detailed structure data is needed for better investigation of such feature in this station. MYG005 station is located in the Onikobe region. The station shows large amplification of factor 5-7 at long- periods of 2-10 s. The area is located in a caldera surrounded by mountains. The thickness of the sedimentary layers is about 900 m. Motoki et al. (2010) studied this area just after the earthquake. They used aftershock data and conducted microtremor measurements in this area. They found a predominant period at 2-3 s at station site and close areas. They concluded that the site amplification is effected not only by 1-D structure, but also by the effects of irregular structure of 4 km in the station area.

We also compared our results with amplification factors obtained by H/H and H/V spectral ratios of the mainshock and five aftershocks (see Table 1). 10 s *S*-wave time windows were chosen for surface and borehole records for calculating of H/H. We define beginning of coda waves as twice the *S*-wave travel time and ends when signal-to-noise spectral ratio is less than 2, following same procedures by Satoh et al., 2001. The resulting values from H/H and H/V are used for comparison with KiK-net stations while the resulting values from H/V are used for comparison with K-NET stations. We picked the maximum value from the spectral curves at each period range of 0.1-0.2, 0.2-0.3, 0.3-0.5, 0.5-1, 1-2, and 2-10 s and plot at the same graph with our amplification results in Figs. 10 and 11. Fig 10 shows the comparison results for KiK-net stations. H/H values of the mainshock and the aftershock data show larger amplification comparing to other results at most stations at short- period ranges of 0.1-0.5 s. The values become closer and smaller at

stations such as IWTH24 and MYGH06 where hard rock sites are expected. Stations such as AKTH06, IWTH04, IWTH22, and MYGH04 show acceleration deamplification at period range of 1-2 s. The values also become closer and smaller at long period ranges. Fig 11 shows the comparison results for K-NET stations. Acceleration and velocity amplification results and H/V results have not shown a systematic difference especially at short periods up to 0.5 s. The values at most stations become closer for periods higher than 0.5 s. Acceleration and velocity amplification for MYG004 station show larger amplification than H/V of the mainshock and aftershocks for all period ranges, while IWT015 station shows opposite results. AKT016 is shown acceleration deamplification at period range of 2-10 s. IWT015 is shown acceleration and velocity deamplifcation at period range of 0.5-2 s. Velocity deamplification is also appeared at some stations such as IWT012 and MYG005 at period ranges of 2-10 s and 0.5-1s, respectively. This deamplification just appeared at results from filtering technique but not at H/H or H/V results. The amplification ratios of acceleration and velocity have shown same tendency but slightly different values at most stations of KiK-net and K-NET. Station such as MYG004, MYG006, and YMT006 are shown larger acceleration amplification than velocity amplification. MYG004 is shown large PGA and PGV amplification at short periods and decrease gradually with period increases. MYG006 is shown approximately flat responses while YMT006 is shown predominant periods at 0.2-0.3 s and 0.3-0.5 s. The stations are located in plain area where deep soft soil structure is expected under these stations. The velocity structure model is available for these stations just for the shallow part down to 10 m for MYG004 and YMT006 and to 20 m for MYG006. Shear wave velocity V_s for MYG004 decreases from 550 m/s to 240 m/s at 6 m depth and decrease again to 100 m/s at 1 m depth. For MYG006, V_s decreases from 400 m/s to 130 m/s at 18 m depth and decrease again to 70 m/s at 2 m depth. While for YMT006, V_s decreases from 120 m/s to 70 m/s at 8 m depth. The difference of V_s velocity structure at each station site can justify the reason of different amplification curves just for short periods. The station sites are located in areas of liquefaction potential. We are not sure if liquefaction occurred at the station sites during the earthquake, however soil non-linear effect should be considered in these sites. Station such as IWT010, IWT011, IWT012 and IWT014 are shown almost same acceleration and velocity amplification values at short and medium periods up to 2 s, while acceleration amplification at these stations is increased than velocity amplification for periods higher than 2 s. The stations are located in plain area where a large river is flowed producing a low land covered with thick sediments (Suzuki et al., 2010).

We also compared our results of H/H and H/V from those by Tsuda et al., 2006. They studied the site response of the 2003 Miyagi-oki earthquake of the mainshock and aftershocks data using a spectral inversion method. The spectrum period range was used in their study is between 0.05-2 s. Our results and their results show same tendency for stations in the Iwate and Miyagi regions in the valid period range of 0.1-2 s. While our results show less values comparing to theirs.

The predominant period of this earthquake is appeared at short period at 0.1 s from acceleration spectral maps (Fig 2). The foot wall area has shown large acceleration amplitudes extended to east direction at 0.1 s as we mentioned previously but not to the hanging wall to the western part of the source area. Low *Q* value to the western part of the source area coming from existence of volcanic front could be the reason of attenuating the short acceleration spectra. But also at a long period of 3 and 5 s large velocity amplitude is observed far to the western part of the source area (Fig 3). The reason might be related to thick sedimentary layer in the Niigata basin.

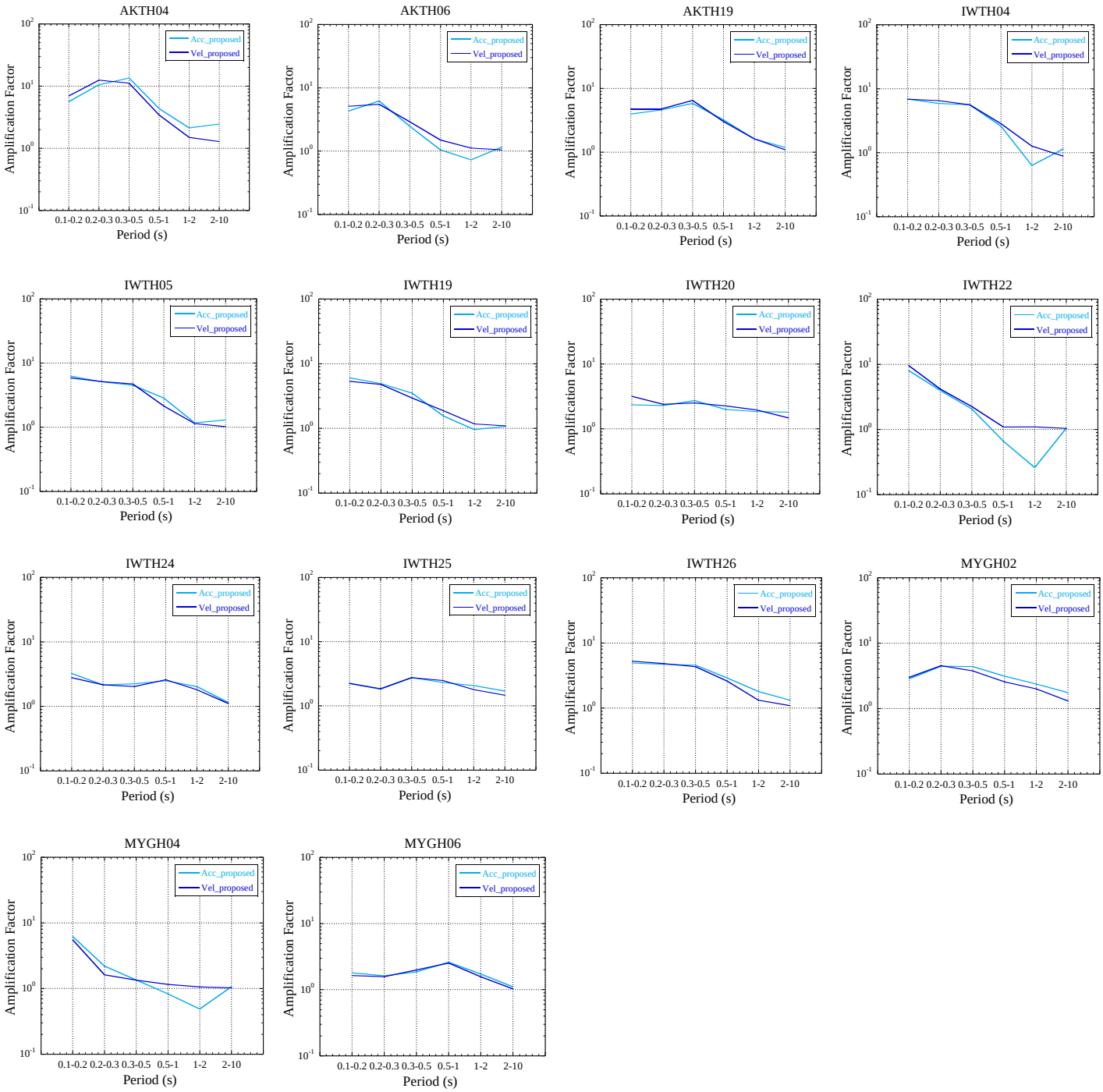

Fig. 8. Light and dark blue curves refer for acceleration and velocity amplification, respectively. Large amplification is dominated for short periods while small amplification for long periods for most stations. Stations such as IWTH20, IWTH24, IWTH25, and MYGH06 show flat and small amplification related to hard rock sites.

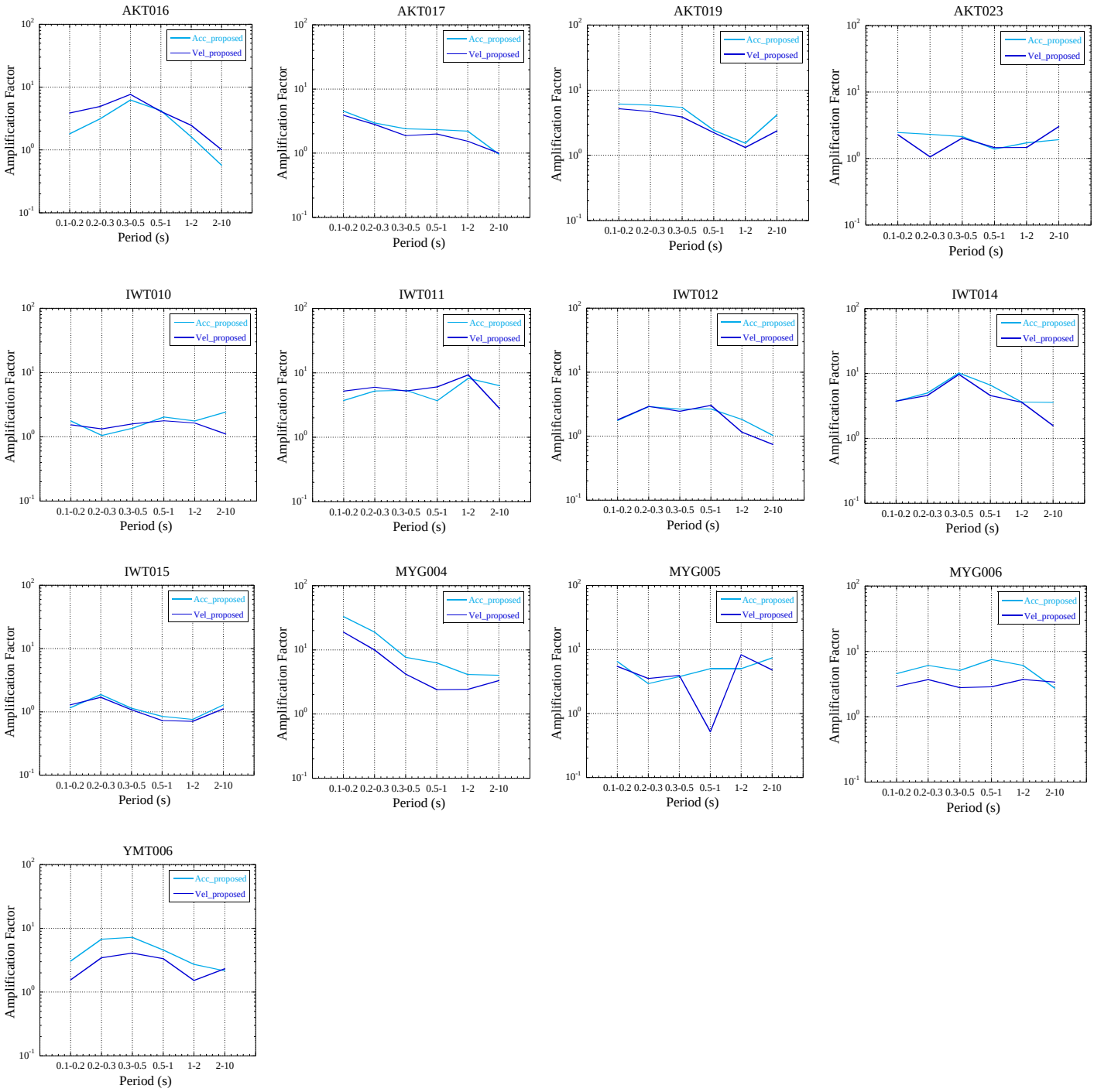

Fig. 9. Light and dark blue curves refer to acceleration and velocity amplification, respectively. Large amplification is dominated for short periods while small amplification for long periods for most stations. Stations such as IWT010, IWT012, and IWT015 show flat and small amplification related to hard rock sites.

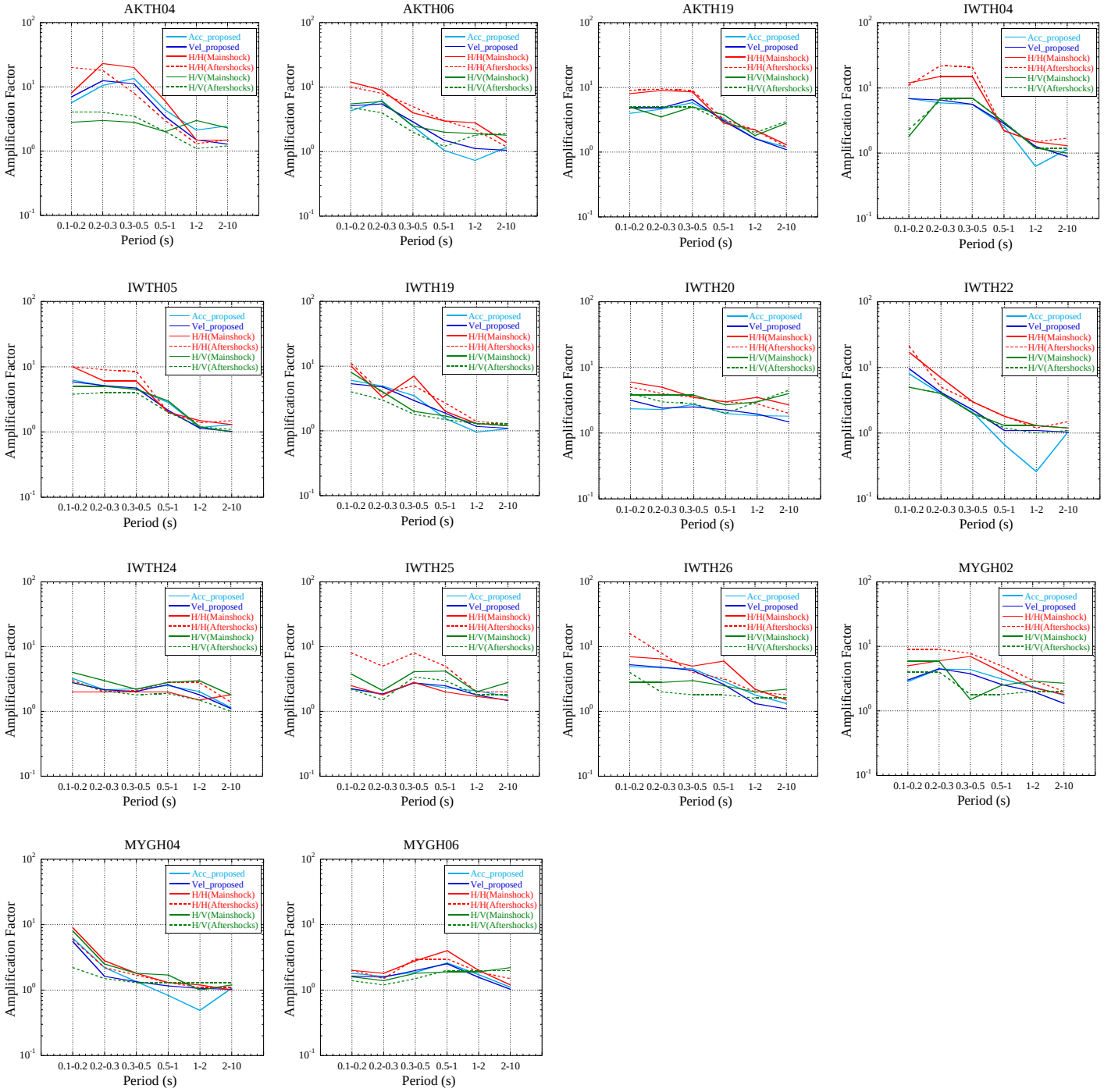

Fig.10. Comparison between acceleration and velocity amplification values obtained by the filtering technique and results from H/H and H/V spectral values for KiK-net stations. The values of H/H and H/V refer to the mainshock and the average value of five aftershocks data. H/H mostly shows larger values comparing with other methods, while H/V shows smaller values.

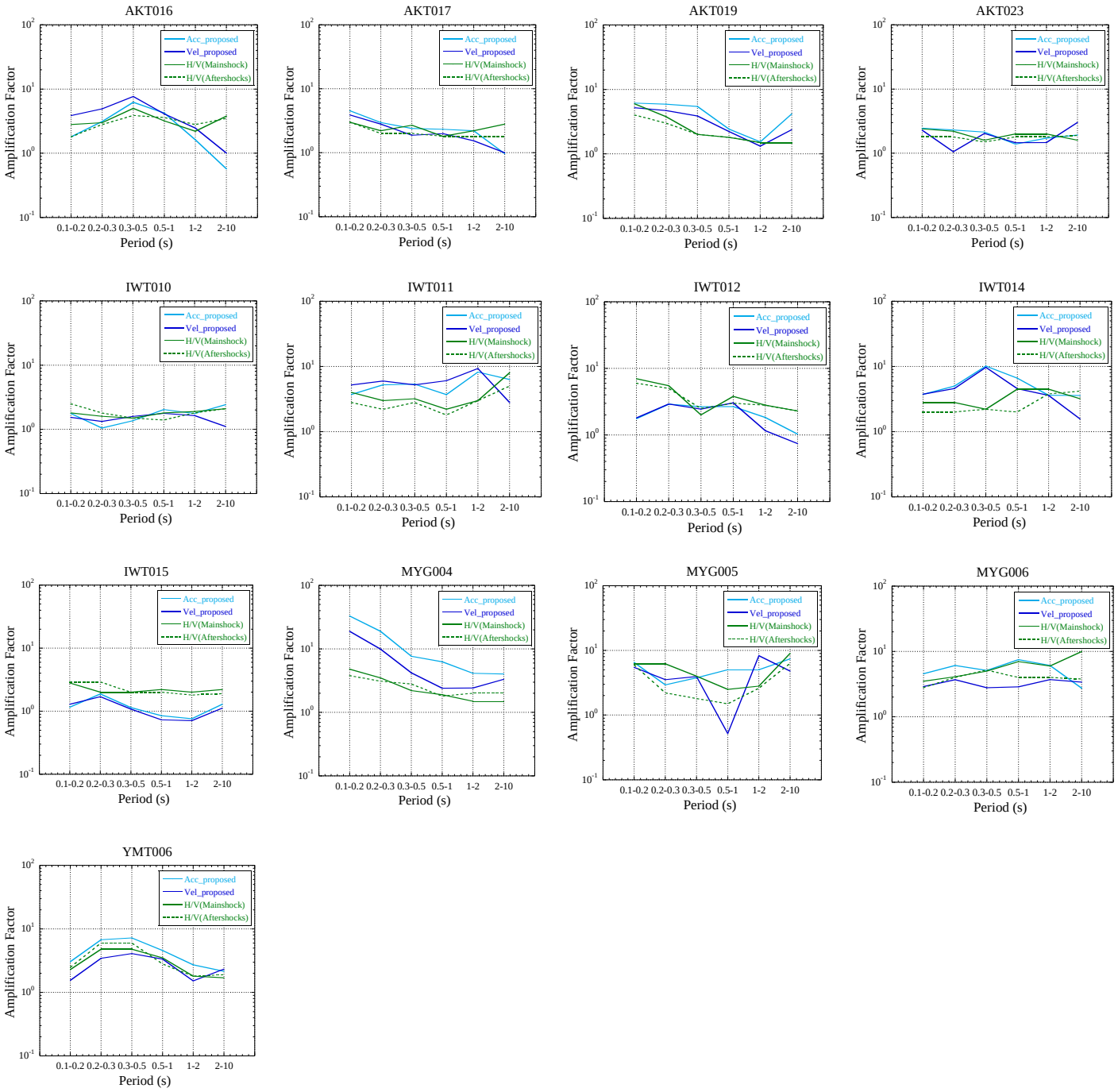

Fig.11 . Comparison between acceleration and velocity amplification values obtained by the filtering technique and results from H/V spectral values for K-NET stations. The values of H/V refer to the mainshock and the average value of five aftershocks.

CONCLUSION

We used borehole stations as reference sites to estimate period-dependent site amplification for uphole and nearby stations. However the effect of the down-going waves was not excluded in this study. The resultant values differentiate between acceleration and velocity amplification. Larger acceleration amplification than velocity amplification is observed in areas where deep soil structure are located. H/H, H/V, and filtering technique results have large amplification but different values at short- periods. Small amplification and close

values at long- periods for most stations. Some stations show small amplifications at most periods related to hard rock sites. We discussed some features of acceleration and velocity response spectral amplitudes which are associated with surface geology.

ACKNOWLEDGMENT

The strong ground motion data of KiK-net and K-NET were provided by National Research Institute for Earth Science and Disaster Prevention (NIED).

REFERENCES

Aki, K. [1993]. “Local site effects on weak and strong ground motion”, Tectonophysics., Vol. 218, pp. 93-111.

Kagami, H., Duke, M., Liang, C. G., and Y. Ohta [1982]. “Observation of 1- to 5-second Microtrmors and their application to earthquake engineering. Part II. Evaluation of site effect upon seismic wave amplification due to extremely deep soil deposits”, Bull. Seismol. Soc. Am., Vol. 72, pp. 987-998.

Kanno, T., Narita, A., Morikawa, N., Fujiwara, H., and Y. Fukushima [2006]. “A new attenuation relation for strong motion in Japan based on recorded data”, Bull. Seismol. Soc. Am., Vol. 96, pp. 879-897.

Kawase, H., and H. Matsuo [2004]. “Amplification characteristics of K-NET, KiK-net, and JMA Shindokei network sites based on the spectral inversion technique”, 13th World Conf. Earthq. Eng., Vancouver, B.C., Canada, No. 454.

Margheriti, L., Wennerberg, L., and J. Boatwright [1994]. “A comparison of coda and S-wave spectral ratios as estimates of site response in the southern San Francisco Bay Area”, Bull. Seismol. Soc. Am., Vol. 84, pp. 1815-1830.

Motoki, K., Yamanaka, H., Seo, K., and H. Suzuki [2010]. “A study of strong motions in the Onikobe area during the 2008 Iwate-Miyagi Nairiku earthquake-Effect of irregular subsurface structure in the Onikobe area from aftershock records and microtremors – (In Japanese), 13th Japan Earthquake Engineering Symposium, pp. 215-222.

Rautian, G. T., and V. I. Khalturin [1978]. “The use of the coda for determination of earthquake source spectrum”, Bull. Seismol. Soc. Am., Vol. 68, pp. 923-948.

Satoh, T., Kawase, H., and S. Matsushima [2001]. “Differences between site characteristics obtained from microtremors, S-waves, P-waves, and codas”, Bull. Seismol. Soc. Am., Vol. 91, pp. 313-334.

Seekins, L., Wenneberg, L., Margheriti, L., and H. Liu [1996]. “Site amplification at five locations in San Francisco, California: A comparison of S-waves, Codas, and Microtremors”, Bull. Seismol. Soc. Am., Vol. 86, pp. 627-635.

Steidl, H. J., Tumarkin, G. A., and R. J. Archuleta [1996]. “What is a reference site?”, Bull. Seismol. Soc. Am., Vol.86, pp. 1733-1748.

Su, F., Aki, K., Teng, T., Zeng, Y., Koyanagi, S., and K. Mayeda [1992]. “The relation between site amplification factor and surficial geology in Central California”, Bull. Seismol. Soc. Am., Vol. 82, pp. 580-602.

Suetomi, I., Ishida, E., Isoyama, R., and Y. Goto [2004]. “Amplification factor of peak ground motion using average shear wave velocity of shallow soil deposits” 13th World Conf. Earthq. Eng., Vancouver, B.C., Canada, No. 448.

Suzuki, W., Aoi, S., and H. Sekiguchi [2010]. “Rupture process of the 2008 Iwate-Miyagi Nairiku, Japan, Earthquake derived from near-source strong-motion records, Bull. Seismol. Soc. Am., Vol. 100, pp. 256-266.

Tsuda, K., Steidl, J., Archuleta, R., D. Assimaki [2006]. “Site response estimation for the 2003 Miyagi-Oki Earthquake sequence considering nonlinear site response”, Bull. Seismol. Soc. Am., Vol. 96, pp. 1474-1482.

Wessel, P., and W.H.F. Smith [1998]. New, improved version of Generic Mapping Tools released, EOS Trans. AGU, 79(47), 579.